Steady Incompressible Navier-Stokes Flow in Curved Two-Dimensional Channels and Three-Dimensional Pipes

Madelyn Bennett[*1], Linnea Helenius[†1], and Shrey Waghmare[#2]

[1]Dept. of Chemical and Biological Engineering, University of Colorado at Boulder
[2]Dept. of Mechanical Engineering, University of Colorado at Boulder

Abstract

Computational Fluid Dynamics (CFD) is a valuable tool for understanding engineering problems that are difficult or expensive to study experimentally. Understanding the fundamentals of a problem allows that knowledge to be applied to many different fields. For example, the flow of fluids in pipes or tubes is relevant to industrial chemical processes, biological systems, heating and cooling, and more. Traditionally, fluid flows are understood through a combination of energy balances (i.e. Bernoulli's equation) and empirical studies. These methods are effective for many macroscopic applications but cannot yield detailed information about the fluid flow and how it behaves at different positions in a pipe. The curvature of a pipe causes interesting local phenomena in fluid flow as well as affecting its overall behavior. To understand the flow of fluids in pipes, this study simulates a steady-state incompressible flow in multiple geometries. First, 2D geometries are considered. Starting with a simpler 2D geometry makes it easier to define the problem, identify critical components such as mesh sizing and computational expense and identify basic trends in the fluid flow. In this report, the effects of inlet flow velocity and channel geometry on overall pressure drop are evaluated. Next, a 3D geometry is simulated, which is more computationally expensive but reveals 3D phenomena such as helicity that are not present in 2D space.

Keywords: Pressure drop, pipe bend, channel flows, computational fluid dynamics

[*]Madelyn.Bennett-1@colorado.edu
[†]Linnea.Helenius@colorado.edu
[#]ShreyRajesh.Waghmare@colorado.edu

1. Introduction

Pipe bends can be found in a variety of engineering applications. Some applications consist of flows in human arteries, chemical piping, HVAC systems and rainwater systems. To initiate flow, there must be a pressure difference. Understanding the pressure drop within a system is imperative to design pumps and the velocity profile within channels or pipes. When using pumps, the pressure drop should be tried to be minimized to save on energy. Bends within a system can be a great cause of pressure drop, so having a good understanding of pressure drop within bends is important.

In 3D pipe bends, vortices occur from an imbalance in centrifugal force and the pressure drop in the radial direction. Secondary circulation starts to occur with the primary flow. Helicity can be used to describe the rotation of flow within a pipe. The Dean number is used to describe these the region in which vortices form in pipe bends. The Dean number is a function of tube diameter, radius of curvature, and Reynolds number.

The turbulent flow regime is a complex system to understand. R. Chiremsel et. al studied an unsteady anisotropic turbulent flow within a 90º pipe bend with a Dean number range of 5000 to 40000 [1]. R. Chiremsel et. al compared the 90º pipe bend with and without ribs and saw that the ribs caused a 47% higher maximum velocity profile. Dixit et. al studied a sand-water slurry through a 90º pipe bend [2]. The addition of solids into the flow caused a higher pressure drop for higher solid concentrations. Multiphysics of flow in pipe bends with heat transfer is also studied using CFD [3]. This project will focus on 90º and 180º channel bends at flow rates ranging from 2 m/s, 20 m/s, and 200 m/s. A 3D 90º pipe bend was also studied to better understand the helicity and vorticity.

2. Numerical method and simulation design

2.1 Numerical method

The problem is described by 2D and 3D steady incompressible flow. The governing equations for this problem are the Navier-Stokes equation for the momentum balance and the continuity equation for the mass balance. The time-dependent terms drop out of both equations because the problem is steady, and the gravitational term is neglected in the Navier-Stokes equation. Navier-Stokes is used instead of Stokes because the Reynolds number is greater than one in all cases tested, meaning that convective momentum transfer is significant (relative to viscous effects).

Momentum Balance: $$\rho \underline{u} \cdot \nabla \underline{u} = -\nabla \underline{p} + \mu \nabla^2 \underline{u} \quad (1)$$

Mass Balance: $$\nabla \cdot \underline{u} = 0 \quad (2)$$

Three geometries (see Figure 1) are considered in this work: a two-dimensional channel with a 90º bend and another with a 180º bend and a 3D pipe with a 90º bend. The channels have the same radius of curvature ($r_c = 1$) but slightly different lengths. The domain, Ω, is defined by its boundary,

Γ (Equation 3).

$$d\Omega = \Gamma = \Gamma_{in} \oplus \Gamma_{left} \oplus \Gamma_{out} \oplus \Gamma_{right} \quad (3)$$

The boundary conditions are a Dirichlet condition for velocity at the inlet, no-slip conditions for velocity at the channel walls, and a Dirichlet zero gauge pressure condition at the outlet.

Boundary Conditions:

$$\underline{u} = \underline{u_D} = [u_{in}, 0] \ \forall x \in \Gamma_{in} \quad (4)$$

$$\underline{u} = \underline{u_D} = [0, 0] \ \forall x \in \Gamma_{left} \oplus \Gamma_{right} \quad (5)$$

$$p = 0 \ \forall x \in \Gamma_{out} \quad (6)$$

The numerical method chosen to solve these equations must account for the instability associated with the nonlinearity of the convective term in the Navier-Stokes equation. To the strong form described by Equations 1-6, the weighted residual method is applied to derive the weak form. A Galerkin discretization is used to convert the weak form to a matrix system. To ensure stability, a Q2P1 element type is used, with a quadratic shape function for the velocity mesh and a linear shape function for the pressure mesh. A Newton solver is used to solve the nonlinear weak form iteratively until the solution converges within an acceptable tolerance.

2.2 Simulation design

For each 2D geometry, three simulations were performed, or six simulations total. The density and viscosity were fixed at one for all simulations. The inlet velocity was changed from 2 m/s, 20 m/s, and 200 m/s causing the Reynolds number and inlet velocity to be equal. The response variable for these experiments was the pressure drop between the channel's inlet and outlet.

Figure 1 shows the 2D meshes that were created for the simulations. A mesh size of 0.05 was created for both geometries. The mesh size was consistent throughout the entire geometry. An unstructured triangular mesh was used.

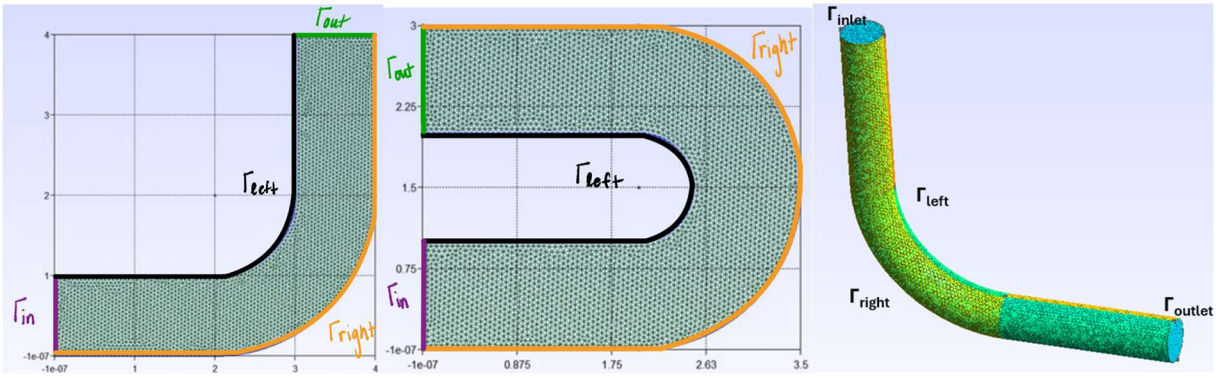

***Figure 1**: 2D Meshes for geometries with a 90º bend (left) and a 180º bend (middle). 3D Mesh for geometry with 90º bend (right).*

The main output variable that was kept track of was pressure drop. The plot over line filter on ParaView 5.12.0-RC2 was used to look at the pressure profile over the inlet and outlet positions. The difference in the pressure profiles between different velocities and geometries were analyzed.

Figure 1 also illustrates the mesh setup for a 3D conduit. In this simulation, an unstructured mesh composed of triangular elements with a size of 0.08 was utilized for the given geometry. The entire computational domain was discretized uniformly. The total number of elements in the mesh were 44000. Boundary conditions employed in this 3D simulation remained consistent with those used in the 2D settings. The simulation was conducted solely for a velocity of 90 m/s owing to increased computational time.

3. Results

The velocity profiles for the six simulations are presented in Figure 2 with the 90º bend and 180º bend with an inlet velocity of 2 m/s. The 20 m/s and 200 m/s cases aren't shown since the profiles look the same qualitatively, but they are in a different order of magnitude. The velocity profile order of magnitude corresponds to 0-3 m/s, 0-30 m/s, and 0-300 m/s for 2 m/s, 20 m/s, and 200 m/s inlet velocities respectively.

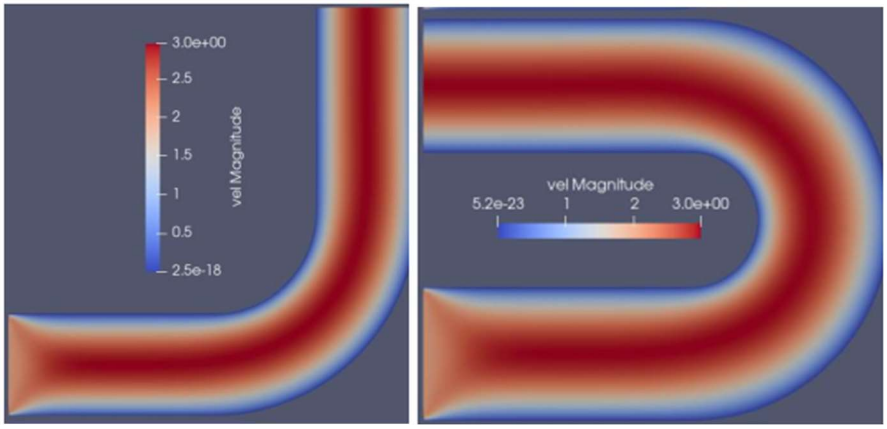

***Figure 2**: Velocity profiles for 2D Meshes: 90º bend with u_{in}=2 m/s (right) and 180º bend with u_{in}=2 m/s.*

The pressure profiles for the six simulations are presented in Figure 3. The columns and rows correspond to the same as Figure 2.

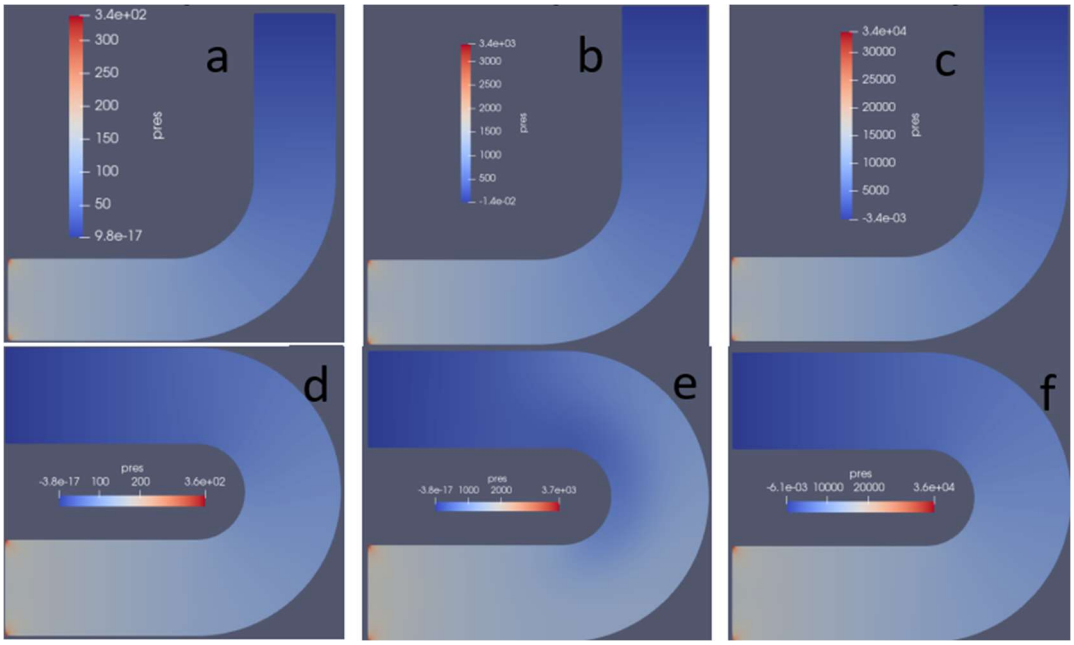

***Figure 3**: Pressure profiles for 2D Meshes: a) 90º bend with u_{in}=2 m/s, b) 90º bend with u_{in}=20 m/s, c) 90º bend with u_{in}=200 m/s, d) 180º bend with u_{in}=2 m/s, e) 180º bend with u_{in}=20 m/s, and f) 180º bend with u_{in}=200 m/s.*

The raw pressure data was extracted, processed, and analyzed. The response variable, pressure drop, was calculated for the experiments. The pressure was taken as a function of position along the channel's diameter at the inlet and outlet. The outlet pressure was then subtracted from the inlet to find pressure drop as a function of position along the channel diameter.

To understand how inlet velocity affects the pressure drop in a 2D channel, the data for the three tested inlet velocities must be compared. First, the data is separated by channel geometry, so the trends viewed in each block will only be a function of inlet velocity. To perform a scaling analysis, which will reveal trends in the data, the pressure drop data for each inlet velocity is reported as a ratio, compared to the pressure drop data for the lowest inlet velocity tested, u_{in} = 2.

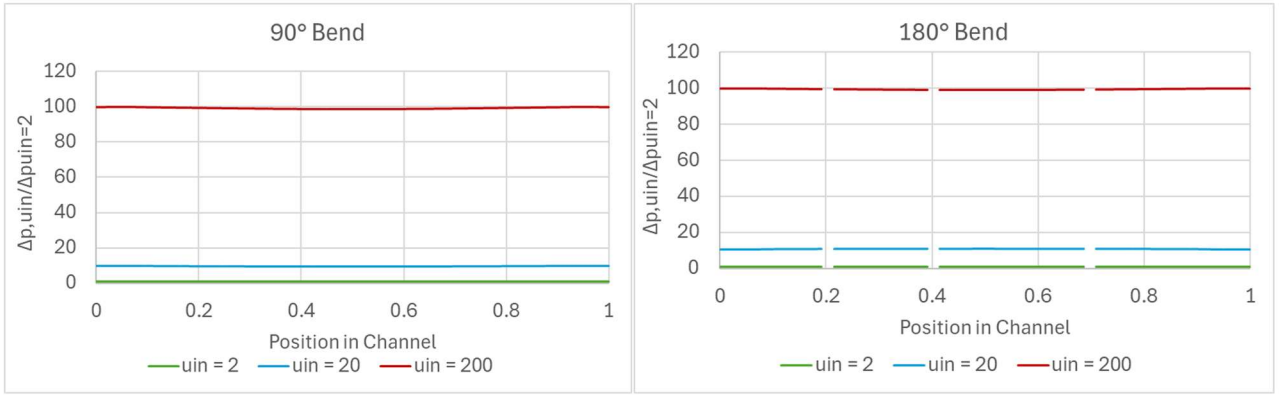

***Figure 4:** Scaled pressure drop results, blocked by geometry to elucidate velocity-driven trends.*

This analysis reveals that the pressure drop increases by a factor of 10 when the inlet velocity increases by a factor of 10, regardless of geometry. This clear linear correlation shows that pressure drop is directly proportional to the inlet velocity. The second variable tested by this experimental design is channel geometry. To compare the channel with the 180º bend to the channel with the 90º bend, their pressure drops are reported as a ratio in Figure 5.

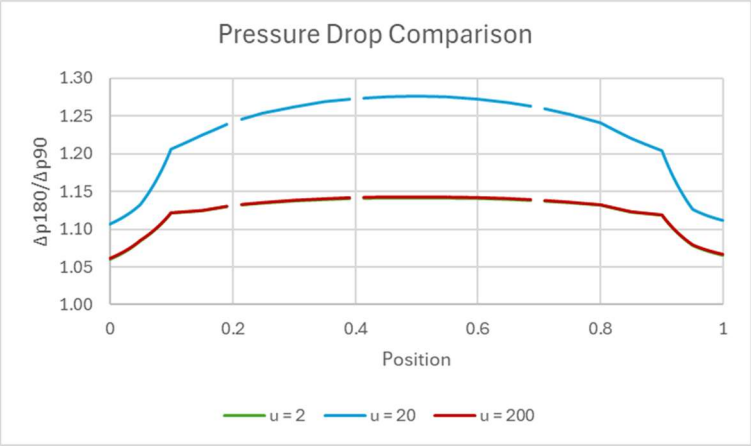

Figure 5: *The relationship between channel geometry and pressure drop is assessed.*

For all three inlet velocities, the pressure drop in the 180º bend channel is at most 14%-28% greater than the 90º bend channel. It is unclear why the $u_{in} = 20$ case has a different ratio than the other two cases. If the channel geometry had the same effect on pressure drop independently of Reynolds number, the results in Figure 5 should be identical among inlet velocities. If there is parity between the Reynolds number and channel geometry, the results would be expected to trend with Reynolds number, but there is not a clear trend, since the high and low velocities had the same results.

A 3D simulation was conducted for the flow case with Re of 90. The Dean number computed for this scenario was 110. To gain deeper understanding on how flow evolves along the curvature, velocity streamlines are also illustrated.

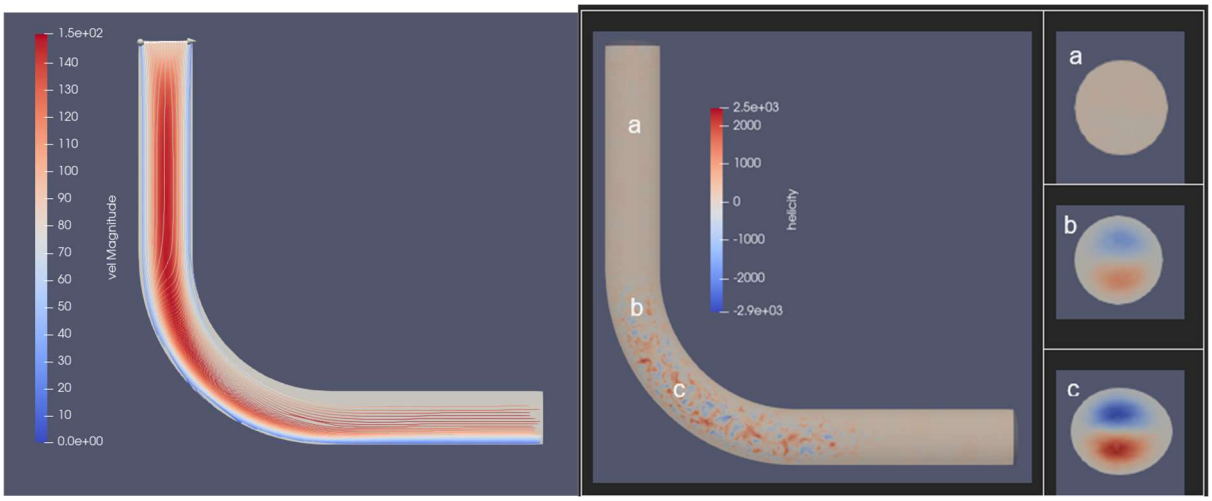

Figure 6: *Velocity streamlines (left) and helicity plots (right).*

At the initial section (0 section), which corresponds to the straight path, the streamlines appear stable. The maximum velocity is observed at the center of cross section. However, as we progress along the curvature, the streamlines become more densely packed towards the outer wall compared to inner wall. Consequently, the maximum velocity shifts towards the outer wall. The bending of streamlines at the curve induces formations of vortices (Dean vortices), a phenomenon elaborated in the later part.

A variety of methods can be used to detect vortex structures within fluid flows, one of which is helicity. The interplay between the primary flow and secondary circulations (vortices) induces a swirling motion of fluid particles, known as helical motion. Flow helicity, defined as the dot product of velocity and vorticity vectors, quantifies this helical motion.

In the current study, secondary flow circulations are visualized using helicity. The helicity plot reveals that at the straight section, no helicity is observed, indicating the absence of vortex formations. However, as we traverse along the curvature, a non-zero helicity value is detected, corresponding to areas where streamlines become crowded, signifying the formation of vortices at the bend section.

A cross-sectional view of helicity is presented at different sections of the pipe. At section 1 (straight section), no helicity is present. At sections 2 and 3, two counter-rotating vortices are evident, with red indicating positive helicity values and blue indicating negative values. The generation of vortices at the curved part is attributed to the presence of centripetal force. This observation aligns with existing literature on vortex formation in curved flows.

4. Discussion

As shown in Figure 2, the velocity profiles for all six simulations show a parabolic profile after the initial constant inlet condition. This was as expected since the Reynolds number was at most 200, so all cases were in the laminar flow regime. For both channel bend cases, the velocity profile order of magnitude increased proportional to the inlet velocity with profiles from 0-3 m/s, 0-30 m/s, and 0-300 m/s corresponding to 2 m/s, 20 m/s, and 200 m/s respectively.

The pressure order of magnitude also scaled with the inlet velocity with 10^2 Pa, 10^3 Pa, and 10^4 Pa corresponding to 2 m/s, 20 m/s, and 200 m/s respectively which is shown in Figure 3. All cases show a similar pressure profile with just the difference in the order of magnitudes. The inlet corners for all cases experience a massive increase in pressure. This is due to two different velocity boundary conditions. The corners are experiencing a constant inlet velocity as well as a no slip boundary condition.

As previously discussed, a linear relationship between inlet velocity and pressure drop was discovered. Without the ability to replicate these tests experimentally, an alternative validation method is to compare these results to generalized empirical relations reported in literature. Flow behavior in pipes is well-studied and well-understood.

The Darcy-Weisbach equation is an empirical relation derived for incompressible, steady, fully-developed flow in a uniform horizontal pipe [4].

$$\Delta p = f \frac{l}{D} \frac{\rho \|u\|^2}{2} \quad (7)$$

Where f is the friction factor, l is the pipe length, D is the hydrodynamic diameter, ρ is the fluid density, and $\|u\|$ is the average fluid velocity.

The channels considered in this report fit the assumptions well, only deviating from fully-developed flow for very short length scales at the inlet. The channels are also 2D, as opposed to a 3D pipe, which affects the aspect ratio (length/diameter). Therefore, this equation is not expected to exactly

replicate the results of the simulation, but it should be able to replicate the scaling analysis.

In the laminar flow regime, the friction factor is only a function of the Reynolds number.

$$f = \frac{64}{Re}; Re = \frac{\rho \|u\| D}{\mu} (8)$$

By substituting the equations for the friction factor (Equation 8) into the Darcy-Weisbach equation (Equation 7), a linear correlation results: $\Delta p \sim \|u\|$. Though the average velocity in the channel varies as a function of position, it is both intuitive and supported by the simulations that the average velocity should be the same order of magnitude as the inlet velocity. Therefore, $\|u\| \sim u_{in}$ and by the transitive property, $\Delta p \sim u_{in}$. This result corroborates the scaling analysis performed based on the simulation data in the Results section.

Validating the channel geometry results is more difficult due to both the inconclusively of the simulation results and the lack of empirical correlations for pressure drop as a function of pipe geometry in literature. Munson, Young, and Okiishi [1] report an equation to calculate “minor losses” caused by geometry, but their loss coefficients were determined for turbulent flow. They do not report equivalent coefficients for laminar flow because they expect flow to be turbulent in most practical cases, and for losses in the laminar flow regime to be inconsequential compared to major losses due to friction (the Darcy-Weisbach equation calculates major losses).

5. Conclusion

In this study, computational fluid dynamics (CFD) simulations were conducted to investigate the behavior of fluid flow in 2D and 3D pipe bends. The focus was on understanding the pressure drop within the system due to bends and variations in inlet velocity. The results showed that the pressure drop is directly proportional to the inlet velocity, regardless of the geometry of the pipe bend. This linear correlation was consistent across all tested inlet velocities and geometries, indicating a clear relationship between inlet velocity and pressure drop. Furthermore, the comparison between different geometries (90° bend and 180° bend) revealed that the pressure drop in the 180° bend channel is slightly greater than that in the 90° bend channel, with a maximum difference of 14%-28%. However, further investigation is needed to understand the underlying factors contributing to this difference, especially regarding the unexpected result for the u_{in} = 20 m/s case. The analysis also included a 3D simulation to understand the vorticity within the flow. The results illustrated the formation of vortices along the curvature, highlighting the complex nature of fluid flow in bends. Overall, the study provides valuable insights into the behaviour of fluid flow in pipe bends and emphasizes the importance of considering factors such as inlet velocity and channel geometry in engineering design and optimization. Additionally, the findings validate theoretical predictions and contribute to the understanding of fluid dynamics phenomena in complex geometries.

References

[1] R. Chiremsel, A. Fourar, F. Massouh, and Z. Chiremsel, “CFD analysis of unsteady and anisotropic turbulent flow in a circular-sectioned 90° bend pipe with and without ribs: A comparative computational study,” *Journal of Mechanical Engineering and Sciences*, vol. 15, no. 2, pp. 7964–7982, Jun. 2021, doi: 10.15282/jmes.15.2.2021.03.0628.

[2] S. Dixit *et al.*, “Numerical simulation of sand–water slurry flow through pipe bend using CFD,” *International Journal on Interactive Design and Manufacturing*, vol. 17, no. 5, pp. 2373–2385, Oct. 2023, doi: 10.1007/s12008-022-01004-x.

[3] K. D. Arvanitis, D. Bouris, and E. Papanicolaou, “Laminar flow and heat transfer in U-bends: The effect of secondary flows in ducts with partial and full curvature,” *International Journal of Thermal Sciences*, vol. 130, pp. 70–93, Aug. 2018, doi: 10.1016/j.ijthermalsci.2018.03.027.

[4] Munson, Young and Okiishi, Fundamentals of Fluid Mechanics, Eighth Edition.